The Von Hippel-Lindau tumor-suppressor protein interaction with protein kinase C delta

Xavier Iturrioz, Joanne Durgan, Véronique Calleja, Banafshé Larijani, Heiwa Okuda, Richard H Whelan, Peter J Parker

Biochemical Journal Immediate Publication. Published on 2 May 2006 as manuscript BJ20060354

THE VON HIPPEL LINDAU TUMOR SUPPRESSOR PROTEIN INTERACTION WITH PROTEIN KINASE C δ.

Xavier Iturrioz‡*, Joanne Durgan‡, Véronique Calleja¶, Banafshé Larijani¶, Heiwa Okuda, Richard Whelan‡ and Peter J. Parker‡§**

‡ Protein Phosphorylation Laboratory and ¶ Cell Biophysics Laboratory, Cancer Research UK London Research Institute, 44 Lincoln's Inn Fields, London, WC2A 3PX, United Kingdom.

**** Department of Urology, Kochi Medical School, Kochi 783-8505, Japan.**

Running Title: pVHL interaction with PKCδ

*Present address: INSERM U691-Collège de France, 11 place Marcelin Berthelot, Paris, 75231, France.

§To whom correspondence should be addressed. Protein Phosphorylation Laboratory, Cancer Research UK London Research Institute, 44 Lincoln's Inn Fields, London WC2A 3PX, United Kingdom. Tel.: 44-20-7269-3018; Fax: 44-20-7269-3094

E-mail: peter.parker@cancer.org.uk

Biochemical Journal Immediate Publication. Published on 2 May 2006 as manuscript BJ20060354

Synopsis

The Von Hippel-Lindau tumor-suppressor protein (pVHL) forms a multi-protein complex (VCB-Cul2) with elongin C, elongin B, Cul-2, and Rbx1, acting as a ubiquitin-ligase (E3) and directing proteasome-dependent degradation of targeted proteins. The α-subunit of hypoxia-inducible factor (Hif1α) is the principal substrate for the VCB-Cul2, however other substrates such as atypical protein kinase C (aPKC) have been reported. In the present study we show by FRET analysis measured by Fluorescence Lifetime Imaging Microscopy that PKCδ and pVHL interact directly in cells. This occurs through the catalytic domain of PKCδ (432-508) which appears to interact with two regions of pVHL, residues 113-122 and 130-154. Despite this robust interaction, analysis of the PMA-induced proteasome-dependent degradation of PKCδ in different renal cell carcinoma lines (RCC4, UMRC2 and 786 O) shows no correlation between the degradation of PKCδ and the presence of an active pVHL. In contrast to aPKC, PKCδ is thus not a conventional substrate of the ubiquitin-ligase complex VCB-Cul2 and the observed interaction between these two proteins must underlie a distinct signaling output.

Abbreviations: VHL, von Hippel-Lindau; pVHL, VHL protein; Hif, hypoxia-inducible factor; PKC, protein kinase C; PMA, phorbol myristate acetate; FRET, Fluorescence Resonance Energy Transfer; FLIM, Fluorescence Lifetime Imaging Microscopy; Y/GFP, yellow/green fluorescent protein; BIM-I, bis-indolylmaleimide-I; RCC, renal cell carcinoma ; VA, vector alone ; GST, glutathione S-transferase.

Biochemical Journal Immediate Publication. Published on 2 May 2006 as manuscript BJ20060354

Introduction

The VHL tumor-suppressor gene is responsible for the inherited familial VHL cancer syndrome and mutations of the VHL gene accompanied by loss of heterozygosity are also found in 70-80% of sporadic clear cell renal carcinomas (RCC) and hemangioblastomas [1]. pVHL has been shown to associate with Elongin C, Elongin B, Cullin-2 (Cul2), and the ring finger protein Rbx1 to form the VCB-Cul2 complex. pVHL has been extensively studied and its most well understood function to date is as a ubiquitin-ligase (E3) specific for hypoxia-inducible factor-1 α (Hif1α), the regulatory subunit of the transcription factor HIF-1 (for review see [2]). In normoxia, Hif 1α is degraded via the ubiquitin-proteasome pathway by an oxygen-dependent mechanism controlled by proline hydroxylases [3-5]. As a consequence of VHL gene inactivation, Hif1α is stabilized and the expression level of vascular endothelial growth factor (VEGF) is increased with subsequent stimulation of angiogenesis. While Hif1α has been the best characterised client of pVHL, it is predicted to be the spectrum of such clients that underlies the distinctive clinical phenotypes associated with specific VHL mutations.

Protein kinase C δ (PKC) belongs to a super-family of lipid-activated serine/threonine kinases, comprising at least 10 different proteins involved in a diverse range of intracellular functions. PKCs are subdivided into three distinct subfamilies (classical, novel and atypical) based upon their mechanism of activation, PKCδ belonging to the novel subfamily (for review see [6]). Activation of classical and novel PKC isoforms induced by tumour promoters of the phorbol ester class (such as PMA), typically leads to their activation and eventual down-regulation; the complex effects of these agents being defined in part by this acute gain and chronic loss of function response. This down-regulation of PKCs, has been reported to be mediated by a ubiquitin/proteasome dependent pathway(s); ubiquitination and degradation of PKCα, δ and ε have been described in rat 3Y1 cells upon chronic activation by phorbol esters [7]. Likewise, ubiquitination of activated PKCζ in HeLa cells [8] and of activated PKCη in baby hamster kidney cells [9] has been observed. More recently, we have shown that PMA- and cell-cycle-induced degradation of PKCδ in NIH3T3 is mediated by poly-ubiquitination of the protein and is dependent on phosphorylation of the activation loop of PKCδ (T505) [10].

PKC isoforms and in particular PKCδ and PKCζ, have been shown to bind pVHL and also to up-regulate VEGF expression by activating mitogen-activated protein kinase (MAPK) in cells that lack pVHL activity [11]. pVHL has been shown to ubiquitinate PKC λ/ι and is to date the only described ubiquitin-ligase showing specificity for a member of PKC family [12]. With respect to PKCδ, evidence has been presented that pVHL is able to inhibit Insulin-like growth factor-I (IGF-I)-mediated cell signaling by directly blocking the association of

PKCδ with IGF-I receptor (IGF-IR) [13]. Moreover, PKCδ has been shown to be activated upon hypoxia and to relay hypoxic signals to HIF-1 and heat shock transcription factor (HSF) in endothelial cells [14].

The above responses provide evidence that PKCδ has a relationship with pVHL and this is of potential importance in that it may inform on the phenotypic diversity of pVHL mutations. However, whether pVHL exerts its action towards PKCδ via its ubiquitin-ligase function and/or as alluded to above, a modulator function towards this protein kinase remains unresolved. In order to probe the pVHL/PKCδ relationship, we have demonstrated the interaction of these proteins in intact cells employing Fluorescence Resonance Energy Transfer (FRET) analysis. We have further mapped the interaction to the catalytic domain of PKCδ and have extended these studies to determine the pattern of interactions for a series of pVHL mutations found in human tumours. The evidence indicates that PKCδ interacts with pVHL via two regions of pVHL. Interactions display a characteristic pattern of behaviour indicative of a role in pVHL mutant class specific phenotypes. To determine whether this pattern of interaction tracks with activation-induced PKCδ downregulation, we have investigated a series of renal cell carcinomas expressing wt or mutant pVHL. The data shows that pVHL does not promote directly the degradation of PKCδ nor does it inhibit the catalytic activity in cells, indicating that distinctive signaling role(s) for this cellular complex are what characterize the interaction.

Experimental

Antibodies: PKCδ-specific antibodies were purchased from Santa Cruz (rabbit polyclonal C-20). PKCε and actin antibodies were obtained from Santa Cruz (rabbit anti-PKCε C-20, goat anti-actin). Hif1α and PKCι-specific antibodies were from BD Transduction Laboratories (mouse monoclonal antibodies). Rabbit anti-PKCζ N terminal antibody was generously provided by Dr T. Sacktor. Mouse anti-α tubulin was purchased from Sigma Aldrich. Polyclonal antisera to the Serine 299 phosphorylation site in PKCδ were raised in rabbits (J.D. and P.J.P. unpublished).

Cell Culture and treatments: Renal carcinoma RCC4, UMRC2 and 786 O cell lines were maintained in DMEM containing 10% FBS, penicillin/Streptomycin and 0.5mg/ml G418. COS7 and 293T were maintained in DMEM containing 10% FBS, Penicillin/Streptomycin. All the cells were cultured at 37°C, 5%CO2. COS7 and 293T were transfected with Lipofectamine 2000 (Invitrogen) according to the manufacturer's instructions.

For the steady state experiments, the RCC4 cells (VA and VHL) were seeded at 25% and 100% confluency and maintained for 48h before harvesting the cells in sample buffer (100mM Tris-HCl pH 6.8, 4% SDS and 20% Glycerol). The amount of protein was determined by BCA assay (Pierce) and protein levels were adjusted to 0.1μg/μl, diluting the sample with water, DTT (1M) and bromophenol blue.

For all the drug treatment experiments RCC4, UMRC2 and 786 O cells (VA and VHL) were seeded at 100% confluency, maintained for 24h to recover and starved overnight with DMEM containing 0.5%FBS. The cells were then treated with 400nM Phorbol 12-Myristate 13-Acetate (PMA) (Sigma) at different times before harvesting all samples in sample buffer 2X (SB2X). For the treatments with drugs such as MG132 (25μM), Calyculin A (10μM), Bisindolylmaleimide I (BIM-I) (10μM), Gö 6976 (1μM) and Rottlerin (Rott) (5μM) (Calbiochem), RCC4 cells were pre-treated for 30min before PMA stimulation and harvested as described.Cell extracts were resolved by SDS-PAGE and proteins were analysed by western blot analysis using specific antibodies.

Plasmid constructs: The VHL open reading frame (ORF) was introduced into pEYFP-C1 or pEGFP-N1 (BD Clontech). YFP-pVHLWT and pVHLWT-GFP constructs were made by amplifying the VHL ORF by PCR, using the flanking primers A) 5'-cggaattctatgccccggagggcggagaac-3' (EcoRI site), B) 5'-gcgggatcctcaatctcccatccgttgatgt- 3' (BamHI site) and C) 5'-cggaattctcataatgccccggagggcggagaac-3' (EcoRI site), D) 5'-ccgggatccgcatctcccatccgttgatgtgc-3' (BamHI site), respectively.

pVHL truncations and deletions were generated using the forward primer C described above (pVHLWT-GFP) and the following primers:

pVHL122-GFP: 5'-gcgggatccgcatctctgaagagccaaaggtg-3' (BamHI site)

pVHL113-GFP: 5'-gcgggatccgctcggtagctgtggatgcggcgcg-3' (BamHI site)

For pVHLΔ87-130-GFP construct, T7 His-pVHLΔ87-130 was used as the PCR template with the pVHLWT-GFP flanking primers C and D.

For pVHL point mutations: Site directed mutagenesis was performed by 2 steps PCR. The forward primer 5'-catgaccttatgggactttcctac-3' and the reverse primer 5'-gctgttgtagttgtactccagc-3' were used with the following specific complementary primers for each mutation (The underlined bases encode the new amino acid residue): pVHLY98H-GFP: 5'-ggcgagccgcagcccc<u>ac</u>ccaacgctgccgcctgg-3' and 5'-ccaggcggcagcgttgggtggggctgcggctcgcc -3'. pVHLC162W-GFP: 5'ctctgaaagagcga<u>tgg</u>ctccaggttgtccg-3'and 5'-cggacaacctggag<u>cca</u>tcgctctttcagag -3'. pVHLR167W-GFP: 5'-gcctccaggttgtct<u>gg</u>agcctagtcaagcctg-3' and 5'- caggcttgactaggct<u>cca</u>gacaacctggaggc -3'.

PKCδ constructs: PKCδ-GST constructs were made using the following oligonucleotides as specific flanking primers for PCR: PKCδ full length GST 5'-gataatacccgggatggcaccgttcctgcgc-3' (Xma I site) and 5'-ctaagcaggtaccgttccaggaattgctcatatttgg-3' (Kpn I site). PKCδ regulatory domain GST 5'-gataatacccgggatggcaccgttcctgcgc-3' (Xma I site) and 5'-gatataaggtaccgccggttgctcccctcccag -3' (Kpn I site). PKCδ catalytic domain GST 5'-gatataacccgggatgctcttggctgaggccttgaacc-3' (Xma I site) and 5'-ctaagcaggtaccgttccaggaattgctcatatttgg-3' (Kpn I site). The PCR products were digested with Xma I and Kpn I restriction enzymes and were cloned into PMT2SM-GST similarly digested.

Truncations of catalytic domain of PKCδ were made by PCR, using the following oligo-nucleotides as forward primers:

CD376 5'-gataatacccgggatgaagtacctgaagaaggacgtggtg-3' (Xma1 site)

CD 432 5'-gataatacccgggatgaaaggccgcttcgaactctacc-3' (Xma1 site)

CD 508 5'-gataatacccgggatggcactcctgactacatcgcccctg-3' (Xma1 site)

CD 616 5'-gataatacccgggatgccgccctttaagcccaaagtgaaatcc-3' (Xma1 site)

The reverse primer was 5'-ctaagcaggtaccgttccaggaattgctcatatttgg-3' (Kpn I site).

Construction of GFP-PKCδ WT, T505/A and K376/M was described previously [10] GFP-PKCδ A147/D was made by site-directed mutagenesis by PCR using the oligo-nucleotides 5'-cggaattcatggcaccgttcctgcgca-3' (EcoRI site) and 5'- gggggtaccctattccaggaattgctcata-3' (KpnI site) as flanking primers and the oligo-nucleotides 5'–cccaactatgaaccgccgtgga<u>gac</u>attaaacaggccaagattcac-3' and 5'-gtgaatcttggcctgtttaat<u>gtc</u>tccacggcggttcatagttggg-3'as complementary mutagenesis primers.

RNA extraction, RT-PCR and sub-cloning of VHL mutants expressed in the RCC4 VA cell line: RNA extraction of RCC4 VA cells was performed with Qiagen RNeasy system following the manufacturer's instructions. Reverse transcription and PCR was performed

using Sigma's SuperScript One-Step RT-PCR with Platinium Taq System with the primers C and D. PCR product was subcloned into pEGFP-N1.

Pull-down and co-immunoprecipitation experiments: 24h post-transfection, cells were harvested in 500µl lysis buffer (50mM Tris-HCl pH 7.5, 150mM NaCl, 0.5 %NP40 or 0.2% CHAPS, 20mM NaF, 2mM EDTA, 2mM EGTA, 2mM Orthovanadate, Protease inhibitors Complete Tablet (Roche)). After 30min incubation on ice and centrifugation at 10,000 rpm for 10min the supernatants were subjected to immunoprecipitation (IP) with rabbit anti-GFP (0.5µl per IP) (BD Clontech) and Protein A Sepharose or pull-down (PD) with Glutathione Sepharose (15µl per PD) (Amersham) and incubated for 2h at 4°C. The beads were washed five times with 1ml of lysis buffer and the final bead pellets were resuspended in 40µl SB2X, boiled and resolved by SDS-PAGE and Western blotting. Immunoreactivity was analysed by chemiluminescence using the ECL system (Amersham).

In vivo poly-ubiquitination assay: 24h post-transfection, HEK 293 cells were pre-treated for 30min with media containing 25μM of MG132 and then the cells were stimulated with 400nM PMA for 30, 60 and 120min. Finally, cells were lysed in 500μl of lysis buffer (50mM Tris-HCl pH 7.5, 150mM NaCl, 1% NP40, 20mM NaF, 2mM EDTA, 2mM EGTA, 2mM orthovanadate, protease inhibitors complete tablet (Roche), 10mM N-ethylmaleimide and 50μM ALLN). After 30 min incubation on ice and centrifugation at 10,0000 rpm for 10 min the supernatants were subjected to immunoprecipitation with mouse anti-HA (3μg per IP) and protein A Sepharose and incubated for 2h at 4°C. The beads were finally washed five times with lysis buffer and the immunoprecipitated proteins were recovered by adding 40μl of SB2X to the last bead pellets and by boiling the beads. The proteins were then resolved by SDS-PAGE and western blot analysis.

Immunofluorescence and Fluorescence Resonance Energy Transfer (FRET): COS7 were transfected with YFP-VHL and PKCδ GST constructs on coverslips. 24h post-transfection the coverslips were fixed with 2% PFA in PBS and after permeabilization and blocking with 0.1% Triton X100, 1% bovine serum albumin (BSA) in PBS, coverslips were incubated with primary rabbit anti-GST (Santa Cruz) (1/250 in PBS 1%BSA) for 1h, washed with PBS and incubated for 45 min with a Cy3-conjugated anti-rabbit (1/500) secondary antibody (Dako). Finally, coverslips were, mounted on slides with Mowiol and examined using a confocal laser scanning microscope (LSM 510, Carl Zeis Inc.) equipped with Krypton/Argon lasers and with 63x/1.4 Plan-APOCHROMAT oil-immersion objective. Double-labeling images (1024x1024 pixels), were analysed in sequential scanning mode by exciting YFP at 488nm and Cy3 at 543nm. For FRET experiments COS7 cells were co-transfected with a 3 to 1 ratio of myc-empty vector/VHL WT-GFP or myc-PKCδ/VHL WT-GFP. 24h post-transfection the cells were fixed for 10min with 4% PFA in PBS. The cells were then permeabilized with

0.2% Triton X100 in PBS for 5min, auto-fluorescence of the cells was quenched with 1mg/ml of Sodium Borohydrate in PBS for 5min and cells were blocked with 1%BSA in PBS for 5min. The cells were then subjected to immunofluorescence (1h) staining with an anti-myc mouse antibody (9E10) (CR-UK) previously labeled with Cy3. Then coverslips cells were mounted with Mowiol containing DABCO.

A detailed description of the FRET monitored by FLIM can be found elsewhere [15, 16]. We monitored lifetime in the frequency (phase) domain; phase methods provide an average lifetime where sinusoidally modulated light is used to excite the sample. The lag in the emitted fluorescence signal permits measurement of phase (τ_p) and modulation depth (τ_m) of the fluorescence. The lifetime, $< \tau >$, is the average of phase shift and relative modulation depth ($\tau_m + \tau_p$) / 2 of the emitted fluorescence signal. All images were taken using a Zeiss Plan-APOCHROMAT 100 x /1.4 numerical aperture, phase 3 oil objective, with images recorded at a modulation frequency of 80.218 MHz. The donor (pVHL-GFP) was excited using the 488 nm line of an Argon/Krypton laser and the resultant fluorescence separated using a combination of dichroic beam splitter (Q 505 LP; Chroma Technology Corp.) and interference filter (HQ510/20 Chroma Technology Corp).

Results and Discussion

Previous studies have shown by co-immunoprecipitation that pVHL interacts with PKCδ [11]. This was initially confirmed through co-immunoprecipitation of HA-pVHL from the renal cell line 786-0 VHL and immunoblot of endogenous PKCδ (see Supplementary Figure) and extended to determine whether the proteins directly interact in intact cells. Shiao *et al*. have shown that pVHL localizes to mitochondria in rat clear cell kidney tumours and that altered pVHL leads to malfunction of this organelle [17]. As previously described, the fusion of YFP at the N-terminus of pVHL WT (Figure 1A) leads to its accumulation in structures surrounding the nucleus (Figure 1B; YFP-pVHL images, green channel); a similar distribution was observed with a dsRed-pVHL construct (data not shown). We have exploited this localisation property to determine whether this form of pVHL is able to recruit different PKCδ GST-tagged constructs into these structures. Expression of full length, regulatory or catalytic domains of PKCδ in COS7 cells, shows a diffuse cytoplasmic staining (Figure 1B red channel). However, when co-expressed with YFP-pVHL the full length and the catalytic domain of PKCδ co-localize with the structures formed by YFP-pVHL (Figure 1B top and bottom images). In contrast, the co-expressed regulatory domain of PKCδ does not co-localize with YFP-pVHL (Figure 1B middle images) demonstrating that the recruitment is specific and not a function of protein co-expression.

Direct pVHL/PKCδ interaction in cells was monitored by Fluorescence Resonance Energy Transfer (FRET) measured by Fluorescence Lifetime Imaging Microscopy (FLIM). This technique determines the lifetime of the donor (pVHL-GFP) such that when the donor interacts with the acceptor (myc-PKCδ immunostained with an anti-myc antibody labeled with the acceptor Cy3) the lifetime of the donor decreases (see [15, 16] for details of the methodologies employed here). Figure 1C shows the image intensities corresponding to the fluorescence intensity of the donor and the τ map, which corresponds to the lifetime $<\tau>$ of the donor (pVHL-GFP). When pVHL-GFP is co-expressed with a myc-empty vector and co-stained with anti-myc-Cy3, the lifetime of the donor corresponds to the lifetime of the GFP. However when co-expressed with myc-PKCδ the observed lifetime decreases significantly demonstrating the existence of FRET between the donor and the anti-Myc-Cy3 acceptor. In Figure 1D the cumulative lifetimes of all pixels recorded for pVHL-GFP/myc empty vector and pVHL-GFP/myc-PKCδ are presented. This two-dimensional histogram shows the lifetimes measured by the two parameters assessed by FLIM (phase and modulation); the concomitant decrease in both indicates a significant decrease in GFP lifetime of the donor due to FRET. This acceptor dependent lifetime decrease indicates close interaction of pVHL and PKCδ in the cytoplasm of intact cells.

To determine the domains of interaction of these two proteins, several deletion

constructs were employed (Figure 2). We found that for PKCδ, the full length and the catalytic domain interact strongly with pVHL-GFP (Figure 2B). Similar results were obtained with a T7-pVHL construct indicating that neither the tag nor the position influence this behaviour (data not shown). To dissect more precisely the interaction of PKCδ with pVHL we further truncated the PKCδ catalytic domain (Figure 2C). GST pull-down experiments (as illustrated in Figure 2D) reveal that truncations 376 CD-GST and 432 CD-GST still interact with pVHL; the shorter truncations of the PKCδ catalytic domain, 508 CD-GST and 616 CD-GST, do not pull-down pVHL. Although the expression level of the 508 truncation is low in this experiment, this was not a consistent observation and at equivalent levels of expression to 376 or 432 there was still no equivalent ability to interact with pVHL. In summary, these results suggest that the domain of interaction of PKCδ with pVHL includes residues between 432 and 508.

As the domain of interaction overlaps the catalytic site of PKCδ and includes the activation loop we investigated if mutants of the catalytic lysine (K376/M) or of the activation loop phosphorylation site T505/A were able to interact with pVHL. We also determined the effect of chronic PMA treatment (24h) on the interaction of wild-type PKCδ with pVHL, as well as the interaction of the constitutively active PKCδ mutant (A147/D) with pVHL. These studies showed that a modest increase of pVHL recovery was observed on PMA treatment, however none of the mutations significantly affect the interaction of PKCδ with pVHL (Figure 3). This indicates that whilst the catalytic domain is sufficient, PKCδ activity *per se* is not required for the pVHL interaction.

For comparison of the mode of interaction of PKCδ and Hif1α with regard to pVHL, a deletion/mutation series of pVHL constructs (See Figure 4A) was tested for interaction with PKCδ; these include deletions of the Hif1α interacting domain (113-122) and mutations that prevent interaction with the Elongin complex (C162W and R167W). Pull-down experiments (Figure 4B and C) reveal that PKCδ binds the truncation 1-122 but not the truncation 1-113 suggesting that the domain of interaction of pVHL with PKCδ includes residues between 113 and 122 as previously reported for the regulatory domain of aPKC [18]. However, the pVHL deletion mutant 87-130 interacts with PKCδ 376 CD-GST, revealing the existence of an additional point of contact. Interestingly, the three hot spot mutations for human VHL syndromes, the Y98H, C162W and R167W, all interact with PKCδ (Figure 4B). This indicates, that mutations which affect Hif1α interaction (as opposed to the elongin C interaction, in particular Δ87-130 and Y98H), may keep their "activity" towards PKCδ.

To further characterize the mode of interaction of pVHL with PKCδ we have isolated the VHL cDNA sequences from RCC4 cells lacking pVHL activity against Hif1α (RCC4 VA). We have thus demonstrated that two mutant alleles are present, namely, S65W and

S65W/Δ114-154 (see Figure 4C). These were sub-cloned into the pEGFP-N1 expression vector and used to determine their ability to bind PKCδ by GST pull-down experiments (Figure 4D). The pVHL S65W mutant interacts with PKCδ whilst the pVHL S65W/Δ114-154 mutant, corresponding to the deletion of the exon 2, loses its ability to bind PKCδ. This result alongside the deletion Δ87-130 data, indicates that the second domain of interaction of PKCδ in pVHL is likely to be located between residues 130 and 154. These results show also that the two domains of interaction (113-122 and 130-154) can act independently. The combination of these two domains may increase the stability of the complex or have a functional activity. Indeed, as noted by Datta et al., the sequence of pVHL comprising residues 113-122 contains a pseudo-substrate-like sequence that is able to inhibit the kinase activity of PKCδ *in vitro* [13].

To determine whether the expression level of PKCδ is influenced by pVHL activity, initially we determined the steady state levels of different PKCs expressed in RCC4 VA or the same cells re-expressing wild-type pVHL (RCC4 VHL). Since Lee et al. have shown that pVHL shuttles between the cytoplasm and nucleus during the cell cycle (being predominantly nuclear in sparsely growing cells and cytosolic in confluent cells) and because the interaction of pVHL with PKCδ occurs in the cytoplasm, we have analysed PKCs expression levels under different culture conditions [19]. Thus, RCC4 cells were seeded at sparse (20% confluent) or high density (100%). Amongst the PKCs tested, only PKCδ shows a significant decrease in the level of expression in RCC4 VHL versus RCC4 VA cells; this is only observed when cells are grown at high density (Figure 5A). PKCε, which like PKCδ belongs to the novel PKC family, shows the opposite expression profile, without any effect of the cell density (Figure 5A). Contrary to expectation, PKCι and PKCζ, which have been shown to be poly-ubiquitinated by pVHL, are modestly up-regulated when wild-type pVHL is expressed and cells cultivated at high density (Figure 5A; see further below). As previously shown, Hif1α expression levels are increased when pVHL activity is lost (Figure 5A). Since Pause et al. have shown that the lack of VHL only affects cell cycle arrest upon serum withdrawal and that cell cycle exit by contact inhibition remains identical in RCC4 and RCC4 re-expressing VHL cells, we can indeed conclude that the effects observed at high density are not a function of a differential ability of these cells to arrest [20]. This decrease in PKCδ expression level only at high density in RCC4 VA cells suggests that pVHL could promote PKCδ downregulation under these conditions and that the presence of pVHL in the cytoplasm is necessary for this degradation. It is of note that no modification of the phosphorylation steady state of PKCδ at S643 and T505 was observable in RCC4 VA and RCC4 VHL cells at different cell densities (Figure 5B).

PMA-induced degradation was also followed in high density RCC4 VA and RCC4 VHL cells, monitoring PKCα, PKCδ and PKCε by western blot (Figure 6A). PMA treatment of RCC4 cell lines shows a down-regulation of all three PKC isoforms, with almost complete loss occurring at 24h of treatment. The involvement of the proteasome in this PMA-induced response was evidenced by its inhibition by co-treatment with MG132. Values obtained by densitometric analysis of different sets of experiments (n=6 for PKCδ and n=5 for PKCα and PKCε) and logarithmic representation of these time courses have been used to determine the rates of degradation (slope of the curves) of PKCs in RCC4 cell lines (Figure 6B). The presence of wild-type pVHL does not affect the rate of degradation of PKCα (0.103 ± 0.027 versus 0.083 ± 0.044 Au/h) and PKCε (0.103 ± 0.035 versus 0.106 ± 0.025 Au/h), but it is associated with a 3 fold ($p<0.05$) increase in the rate of degradation of PKCδ (0.085 ± 0.034 versus 0.306 ± 0.032 Au/h). These results suggest that pVHL might promote the degradation of PKCδ and that this degradation is under the control of the ubiquitin-proteasome system. *In vivo* poly-ubiquitination assays of PKCδ co-expressed with pVHL and HA-tagged ubiquitin in 293T cells, confirms ubiquitin-ligase activity of pVHL towards PKCδ under over-expression conditions (Figure 6D).

We have shown previously that the downregulation of PKCδ during cell cycle progression is dependent on the phosphorylation of the activation loop at threonine 505 (T505) and can be promoted by calyculin A, a PP2A selective inhibitor, and inhibited by the PKC inhibitor BIM-1 [10]. This pattern of behaviour is only partially retained in the RCC4 lines (Figure 5D). Co-treatment of RCC4 cells with calyculin A does not inhibit PKCδ degradation, while inhibition of PKCδ with BIM-1 or Rottlerin but not the more PKCα selective Gö 6976, blocks PMA-induced degradation of PKCδ in both cell lines. It should be noted that Gö 6976 was effective in blocking PMA-induced PKCα degradation. The results indicate that while the presence of wild-type pVHL is associated with increased PMA-induced degradation of PKCδ, the degradation in these renal cell carcinomas requires a functional kinase activity, clearly contrasting with the requirement for pVHL-PKCδ interaction (see above).

The distinction in behaviour of the PMA-induced PKCδ downregulation and pVHL interaction questioned whether the RCC4 ± pVHL effects were clonal variations or a reflection of an independent function for the interaction. Since direct siRNA knock-down of pVHL in the RCC cells lines has not been possible (data not shown), we investigated this issue by analysis of two other renal cell carcinomas that retain or lack pVHL activity. Specifically the UMRC2 (VA and VHL) and the 786 O (VA and VHL) lines were employed to determine steady state PKCδ levels and also its degradation behaviour in these cell lines (Figure 7). UMRC2 VA present a weak expression of a mutated pVHL form, whereas the

786 O VA cell line lacks detectable pVHL expression. In contrast to the results obtained with the RCC4 cell lines, the presence of pVHL in UMRC2 or 786 O cell lines does not change the steady state of PKCδ (the concentrations being assessed as a function of tubulin expression). In respect of the steady state behaviour of atypical PKCs, we note that the effect of pVHL expression does not correlate with the overall level of protein, rather with the relative accumulation of the dephosphorylated form of the protein. The low abundance of the shifted, phosphorylated aPKC form makes it impossible to determine whether the loss of this upper phosphorylated form is directly related to the increase of the lower or not, i.e. whether the apparent effect of pVHL is degradation of the phosphorylated form as proposed elsewhere [21] or dephosphorylation of the pVHL associated kinase.

For PMA-induced degradation of PKCδ, this is significantly increased in UMRC2 VA by comparison with the UMRC2 VHL; there is a modest and equivalent degree of PMA-induced degradation in the 786 O VA and VHL cells (Figure 7B). These results demonstrate that there is no correlation between the presence of active pVHL and the induced degradation of PKCδ in these renal carcinoma cell lines. It is evident that pVHL is not required for the activation-induced downregulation of PKCδ and that the differences in PKCδ degradation observed between these renal cell carcinoma lines are most likely due to clonal variations. Similarly comparison of the levels of PKCδ in the three pairs of renal cell lines indicates that there is also no correlation of PKCδ steady state levels with VHL expression.

The lack of a requirement for pVHL in the PMA-induced downregulation and steady state turnover of PKCδ juxtaposed to the clear demonstration of complex formation in cells, supports the notion that through this interaction pVHL influences PKCδ activity. Two different studies have indeed reported such functions. Pal et al. have demonstrated that pVHL can block translocation to cell membranes of PKCζ and PKCδ, blocking activation and preventing a signaling step that leads to VPF/VEGF expression [11]. Datta et al. have shown that PKCδ kinase activity *in vitro* can be inhibited by pVHL-derived peptides and that in the context of IGF-I signaling, pVHL can inhibit PKCδ association with IGF-1R, decreasing the invasiveness of the cells expressing pVHL [13]. These effects of complex formation on PKCδ function/activity indicate that the key role of the interaction is in tempering the immediate functional output of PKCδ rather than the more characteristic function of pVHL i.e. the induced degradation of the associated protein. To assess whether this was a direct effect on PKCδ activity effected through the in vitro defined inhibitory effect of pVHL [13], we monitored PKCδ activity in intact cells employing a novel autophosphorylation site (manuscript in preparation). PMA-induced phosphorylation of PKCδ at the serine 299 site was not significantly affected by the presence or absence of pVHL (Figure 8). The lack of effect of pVHL on PKCδ activity juxtaposed to the non-involvement in the PKCδ down-

regulation pathway indicates that the functional effect is likely to be directed at a specific substrate(s) perhaps mediated through localisation.

PKCδ has been implicated in cell cycle regulation and apoptosis in many different cell types. The extent to which these properties contribute to the pattern of pVHL associated disease progression remains to be determined. However it is now clear that this will not be reflected simply in the altered turnover of PKCδ, nor through direct inhibition, but rather through altered localisation and/or selective substrate targeting. This distinction is important as it determines the nature of the parameters required for an assessment of whether PKCδ contributes to VHL disease sub-classes in the clinical setting.

Acknowledgments

We would like to thank Dr Peter Ratcliffe and Dr. Norma Masson for RCC4, UMRC2 and 786 O cell line.

References

1 Barry, R. E. and Krek, W. (2004) The von Hippel-Lindau tumour suppressor: a multi-faceted inhibitor of tumourigenesis. Trends Mol Med **10**, 466-472

2 Kim, W. Y. and Kaelin, W. G. (2004) Role of VHL gene mutation in human cancer. J Clin Oncol **22**, 4991-5004

3 Ivan, M., Kondo, K., Yang, H., Kim, W., Valiando, J., Ohh, M., Salic, A., Asara, J. M., Lane, W. S. and Kaelin, W. G., Jr. (2001) HIFalpha targeted for VHL-mediated destruction by proline hydroxylation: implications for O2 sensing. Science **292**, 464-468

4 Yu, F., White, S. B., Zhao, Q. and Lee, F. S. (2001) HIF-1alpha binding to VHL is regulated by stimulus-sensitive proline hydroxylation. Proc Natl Acad Sci U S A **98**, 9630-9635

5 Jaakkola, P., Mole, D. R., Tian, Y. M., Wilson, M. I., Gielbert, J., Gaskell, S. J., Kriegsheim, A., Hebestreit, H. F., Mukherji, M., Schofield, C. J., Maxwell, P. H., Pugh, C. W. and Ratcliffe, P. J. (2001) Targeting of HIF-alpha to the von Hippel-Lindau ubiquitylation complex by O2-regulated prolyl hydroxylation. Science **292**, 468-472

6 Mellor, H. and Parker, P. J. (1998) The extended protein kinase C superfamily. Biochem J **332 (Pt 2)**, 281-292

7 Lu, Z., Liu, D., Hornia, A., Devonish, W., Pagano, M. and Foster, D. A. (1998) Activation of protein kinase C triggers its ubiquitination and degradation. Mol Cell Biol **18**, 839-845

8 Smith, L., Chen, L., Reyland, M. E., DeVries, T. A., Talanian, R. V., Omura, S. and Smith, J. B. (2000) Activation of atypical protein kinase C zeta by caspase processing and degradation by the ubiquitin-proteasome system. J Biol Chem **275**, 40620-40627

9 Kang, B. S., French, O. G., Sando, J. J. and Hahn, C. S. (2000) Activation-dependent degradation of protein kinase C eta. Oncogene **19**, 4263-4272

10 Srivastava, J., Procyk, K. J., Iturrioz, X. and Parker, P. J. (2002) Phosphorylation is required for PMA- and cell-cycle-induced degradation of protein kinase Cdelta. Biochem J **368**, 349-355

11 Pal, S., Claffey, K. P., Dvorak, H. F. and Mukhopadhyay, D. (1997) The von Hippel-Lindau gene product inhibits vascular permeability factor/vascular endothelial growth factor expression in renal cell carcinoma by blocking protein kinase C pathways. J Biol Chem **272**, 27509-27512

12 Okuda, H., Saitoh, K., Hirai, S., Iwai, K., Takaki, Y., Baba, M., Minato, N., Ohno, S. and Shuin, T. (2001) The von Hippel-Lindau tumor suppressor protein mediates ubiquitination of activated atypical protein kinase C. J Biol Chem **276**, 43611-43617

13 Datta, K., Nambudripad, R., Pal, S., Zhou, M., Cohen, H. T. and Mukhopadhyay, D. (2000) Inhibition of insulin-like growth factor-I-mediated cell signaling by the von Hippel-Lindau gene product in renal cancer. J Biol Chem **275**, 20700-20706

14 Baek, S. H., Lee, U. Y., Park, E. M., Han, M. Y., Lee, Y. S. and Park, Y. M. (2001) Role of protein kinase Cdelta in transmitting hypoxia signal to HSF and HIF-1. J Cell Physiol **188**, 223-235

15 Squire, A. and Bastiaens, P. I. (1999) Three dimensional image restoration in fluorescence lifetime imaging microscopy. J Microsc **193 (Pt 1)**, 36-49

16 Larijani, B., Allen-Baume, V., Morgan, C. P., Li, M. and Cockcroft, S. (2003) EGF regulation of PITP dynamics is blocked by inhibitors of phospholipase C and of the Ras-MAP kinase pathway. Curr Biol **13**, 78-84

17 Shiao, Y. H., Resau, J. H., Nagashima, K., Anderson, L. M. and Ramakrishna, G. (2000) The von Hippel-Lindau tumor suppressor targets to mitochondria. Cancer Res **60**, 2816-2819

18 Okuda, H., Hirai, S., Takaki, Y., Kamada, M., Baba, M., Sakai, N., Kishida, T., Kaneko, S., Yao, M., Ohno, S. and Shuin, T. (1999) Direct interaction of the beta-domain of VHL tumor suppressor protein with the regulatory domain of atypical PKC isotypes. Biochem Biophys Res Commun **263**, 491-497

19 Lee, S., Chen, D. Y., Humphrey, J. S., Gnarra, J. R., Linehan, W. M. and Klausner, R. D. (1996) Nuclear/cytoplasmic localization of the von Hippel-Lindau tumor suppressor gene product is determined by cell density. Proc Natl Acad Sci U S A **93**, 1770-1775

20 Pause, A., Lee, S., Lonergan, K. M. and Klausner, R. D. (1998) The von Hippel-Lindau tumor suppressor gene is required for cell cycle exit upon serum withdrawal. Proc Natl Acad Sci U S A **95**, 993-998

21 Lee, S., Nakamura, E., Yang, H., Wei, W., Linggi, M. S., Sajan, M. P., Farese, R. V., Freeman, R. S., Carter, B. D., Kaelin, W. G., Jr. and Schlisio, S. (2005) Neuronal apoptosis linked to EglN3 prolyl hydroxylase and familial pheochromocytoma genes: developmental culling and cancer. Cancer Cell **8**, 155-167

Figure Legends

Figure 1: Interactions of PKCδ with pVHL in cells. A, schematic representation of the YFP-pVHL construct. B, Immunofluorescence analysis of COS7 cells co-transfected with YFP-pVHL and three different GST constructs of PKCδ (see Materials and Methods). Images represent a confocal equatorial section of the cells. C, COS7 cells were co-transfected with pVHL-GFP/myc empty vector or pVHL-GFP/myc-PKCδ. Myc expression was detected with an anti-myc mAb directly labeled with Cy3 and interaction of pVHL-GFP with myc-PKCδ was analysed by FRET measured by FLIM. The top images correspond to the image intensity of the donor and the bottom images represent the lifetime ($< \tau >$) of GFP shown with pseudocolor scales from red (1.8ns) to blue (2.5ns). D, Two-dimensional histograms of (τ p) and (τ m) lifetimes obtained in the frequency domain illustrating the variation in lifetime in three independent experiments. pVHL-GFP/myc empty vector (white), VHL-GFP/myc-PKCδ (red).

Figure 2: Characterization of PKCδ interaction with pVHL. A, Schematic representation of PKCδ GST constructs, T7-pVHL WT and pVHL WT-GFP fusion proteins used in pull-down experiments. B, COS7 cells were co-transfected with GST alone (-), PKCδ full length (FL), regulatory (RD) or catalytic (CD) domain GST fusion proteins and pVHL WT-GFP. The interaction with pVHL-GFP is evidenced in the central panel. C, Schematic representation of PKCδ catalytic GST tagged mutations and truncations. The K376 and T505 correspond to the ATP binding site and the T-loop site respectively. The results of 3 different pull-down experiments are summarized on the right hand side. D, COS 7 cells were co-transfected with truncation constructs of the PKCδ catalytic domain and pVHL WT-GFP. Cell extracts were subjected to a pull-down experiment on GST-beads and protein complexes were resolved by SDS-PAGE and western blot analysis with anti-GST antibodies for the PKCd truncations anti-GFP for pVHL recovery.

Figure 3: pVHL interaction with mutants of PKCδ. 293T cells stably expressing T7-pVHL WT, were co-transfected with wild type PKCδ and PKCδ mutants (A147/D, K376/M and T505/M). Co-transfections with wild type PKCδ were treated with or without 400nM PMA for 24h. After 48h transfection the cells were lysed and subjected to immunoprecipitation with a rabbit anti-GFP antibody and protein complexes were resolved by SDS-PAGE and immunoblot analysis.

Figure 4: Analysis of the interactions of mutants of pVHL with PKCδ. A, schematic representations of pVHL constructs. B, COS7 cells were co-transfected with pVHL-GFP constructs and CD 376 PKCδ-GST or GST empty vector. C, schematic representation of constructs of pVHL containing the two defined allelic mutations present in RCC4 VA cells. D, COS 7 cells were co-transfected with CD 376 PKCδ-GST or GST empty vector and wild type or mutated pVHLs. B and D Cells were then lysed and protein complexes were purified by GST pull-down and analysed by SDS-PAGE and western blot analysis.

Figure 5: Analysis of PKCδ turnover and phosphorylation by pVHL. A, Steady state protein levels of different protein kinases C in RCC4 VA and RCC4 VHL cell lines (cell extracts: 4μg for Hif1α, PKCα and PKCε, 2μg for PKCι and ζ and 1μg for PKCδ and actin) (see Materials and Methods). Densitometric analysis of the steady state protein levels of protein kinase Cs in RCC4 VA and RCC4 VHL cells at different cell densities is included below. B, The steady state phosphorylation of PKCδ was determined for the activation loop T505 site and the C-terminal turn motif site S643. Graphic: Densitometric analysis of the steady state phosphorylation of PKCδ in RCC4 VA and RCC4 VHL for T505 and S643. HD, high density; LD, low density.

Figure 6: PKCδ down-regulation in RCC4 cells. A. PMA-induced degradation of PKCs in high density RCC4 VA and RCC4 VHL cell lines. B, Logarithmic representations of the PMA-induced degradation time courses of different protein kinase Cs obtained in RCC4 cell lines. C, The effect of CalA (10nM), Bim I (10μM), Gö 6976 (1μM) and Rottlerin (5μM) on PMA-induced degradation of PKCα and PKCδ in RCC4 cell lines. D. pVHL promotes poly-ubiquitination of PKCδ. HEK293 transfected cells were treated for different times with 400nM PMA in presence of MG132 (16μM) and cells were then lysed in poly-ubiquitination buffer and subjected to immunoprecipitation with an anti-HA Rabbit antibody (Santa Cruz). Proteins were then resolved by SDS-PAGE and myc-PKCδ was analysed with an anti-PKCδ (Santa Cruz) antibody.

Figure 7: Analysis of PKCδ degradation in UMRC2 and 786 O cell lines with or without pVHL. A, Steady state protein levels of different protein kinase Cs in UMRC2 and 786 O. Steady state

protein levels of different protein kinases Cs in confluent UMRC2 and 786 O cell lines (cell extracts: 80μg for PKCα, 60μg for PKCε, 2μg for PKCζ and tubulin and 1μg for PKCδ). B, PMA-induced degradation of PKCs in high density UMRC2 (VA and VHL) and 786 O (VA and VHL).

Figure 8: pVHL does not inhibit PKCδ autophsophorylation in 786 O cells. Cells were allowed to approach confluency and then switched to 0.5%FCS in DMEM overnight. Cells were then either treated with vehicle (0.1% ethanol) or PMA (1μM) for 15 minutes. Extracts were prepared and blotted for PKCδ protein (upper panel) and for the induced autophosphorylation of serine 299 in the presence of the dephosphopeptide to suppress any recognition of the dephosphorylated site (middle panel) or both dephospho- and phospho-peptides to demonstrate the specificity of immunodetection (lower panel). This is one of two consistent experiments. The asterisks denote non-specific immunoreactions.

Biochemical Journal Immediate Publication. Published on 2 May 2006 as manuscript BJ20060354

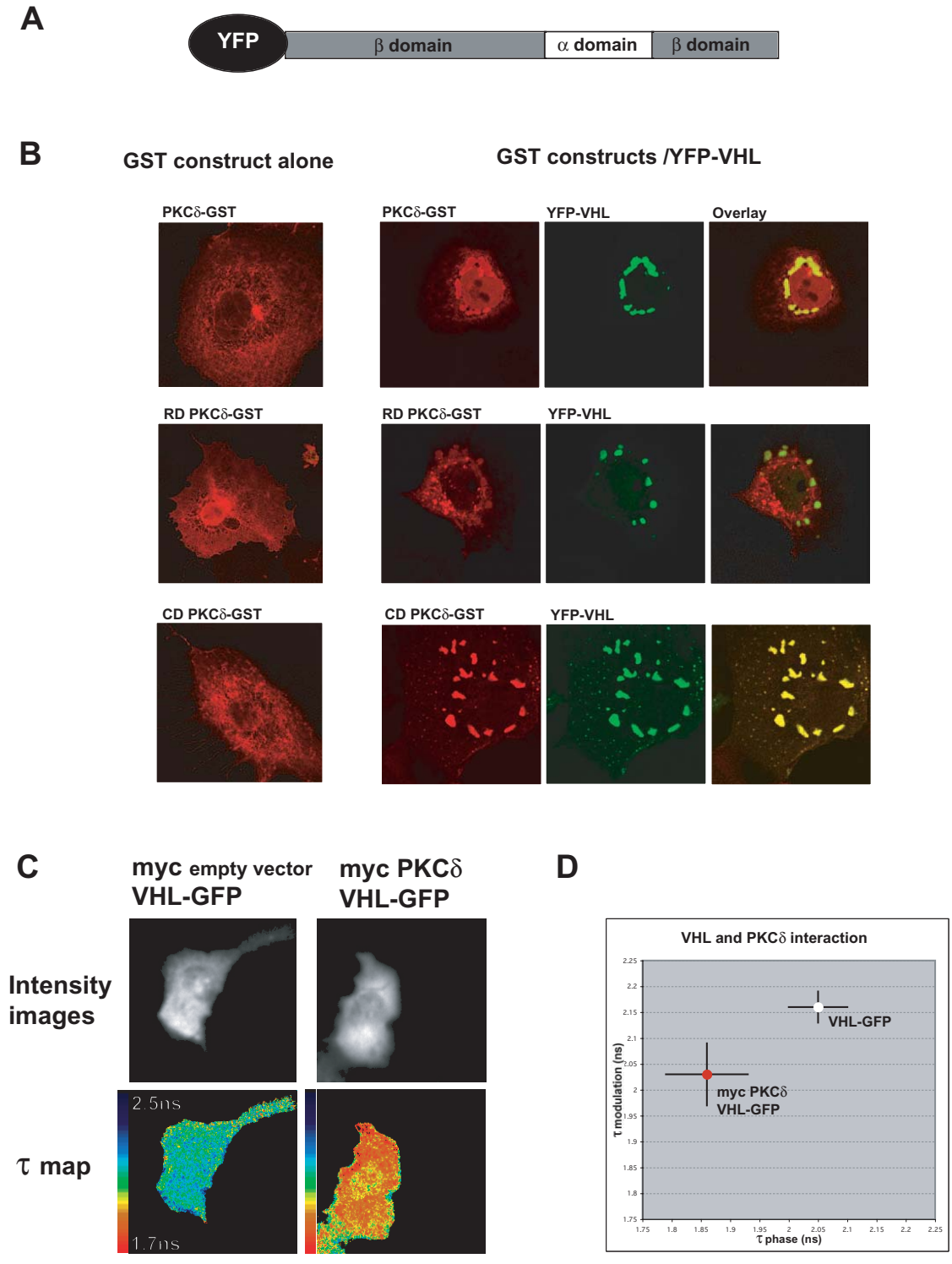

Iturrioz et al. Figure 1

Biochemical Journal Immediate Publication. Published on 2 May 2006 as manuscript BJ20060354

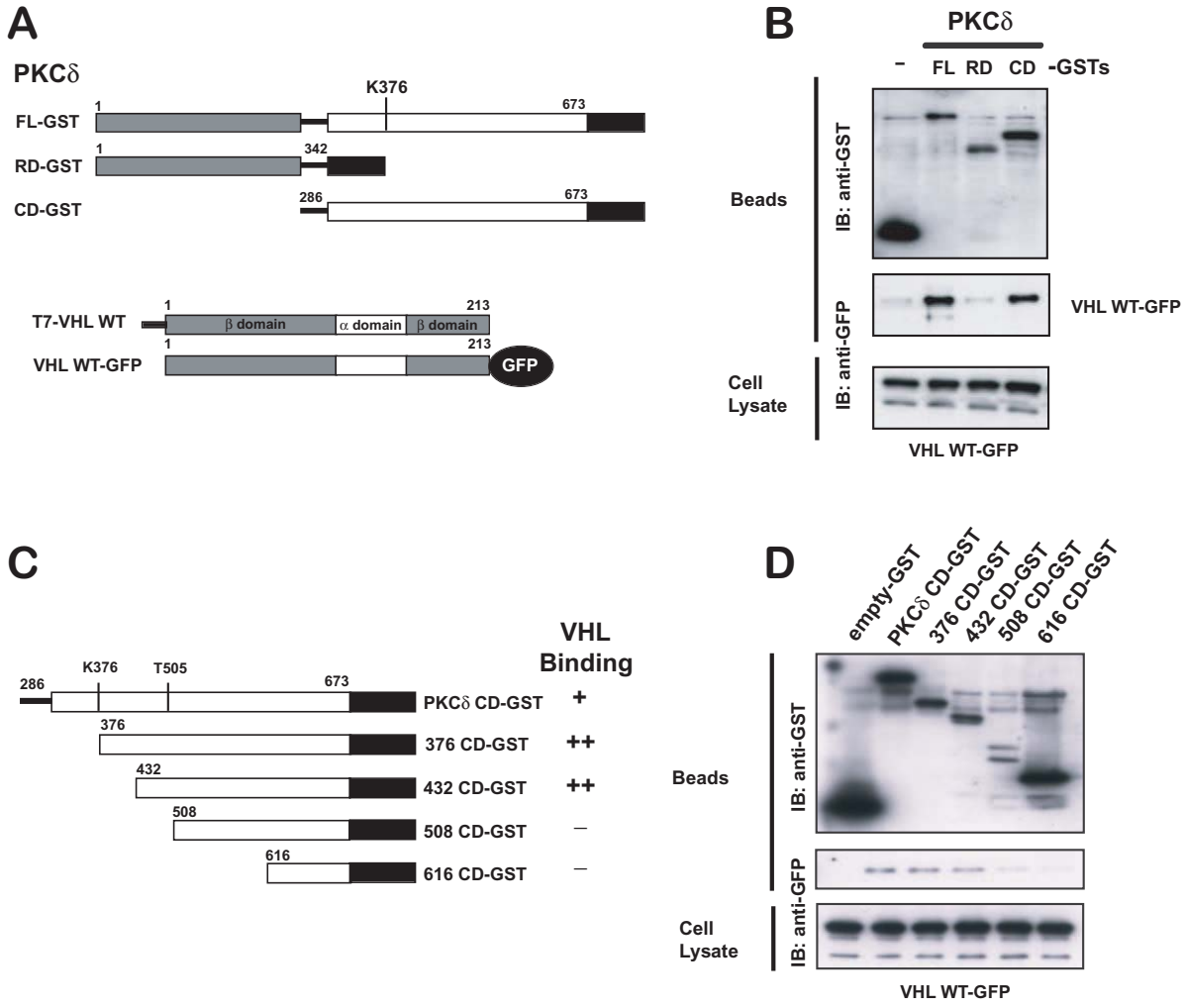

Iturrioz et al. Figure 2

Biochemical Journal Immediate Publication. Published on 2 May 2006 as manuscript BJ20060354

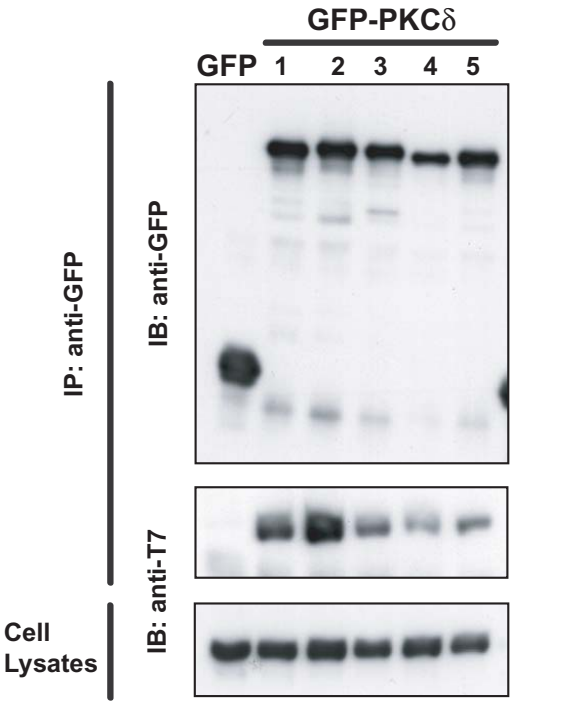

1: GFP-PKCδ WT
2: GFP-PKCδ WT + TPA 400nM (24h)
3: GFP-PKCδ A147/D
4: GFP-PKCδ K376/M
5: GFP-PKCδ T505/A

Iturrioz et al. Figure 3

Biochemical Journal Immediate Publication. Published on 2 May 2006 as manuscript BJ20060354

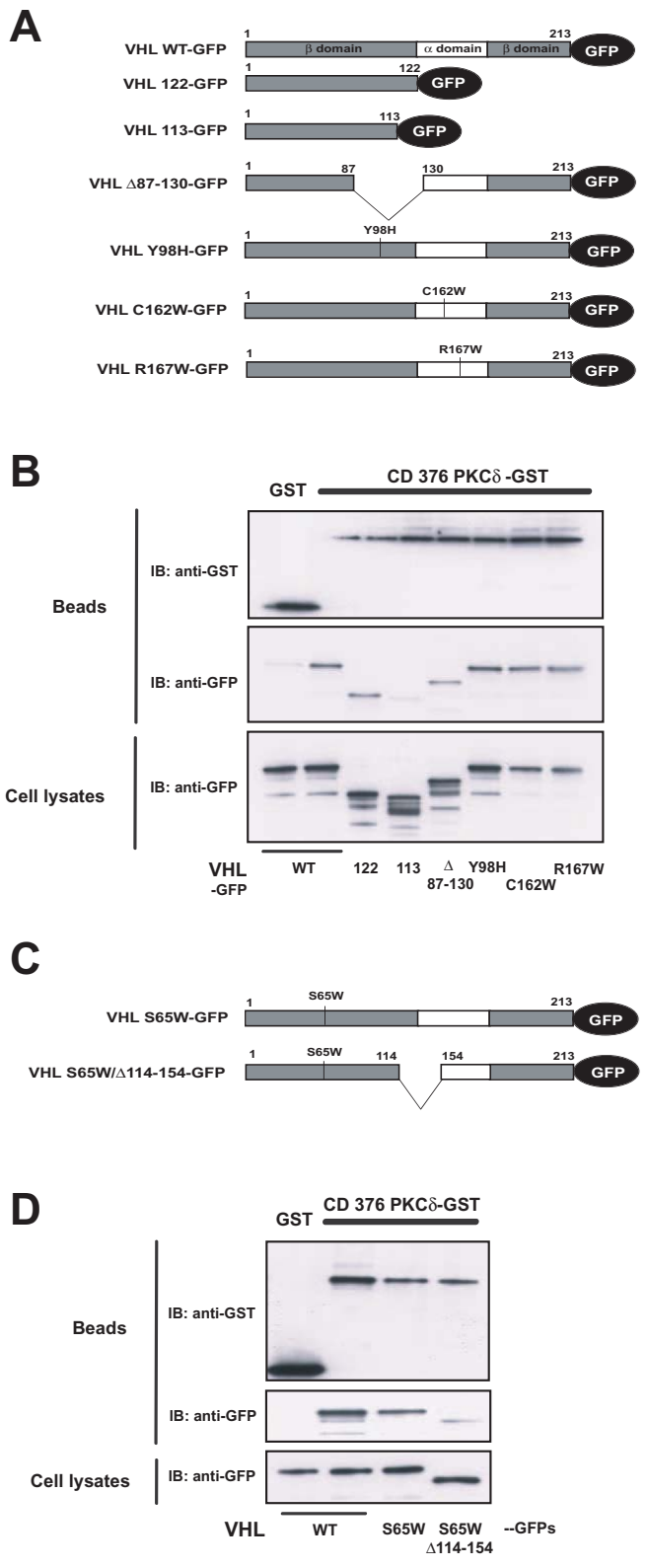

Iturrioz et al. Figure 4

Biochemical Journal Immediate Publication. Published on 2 May 2006 as manuscript BJ20060354

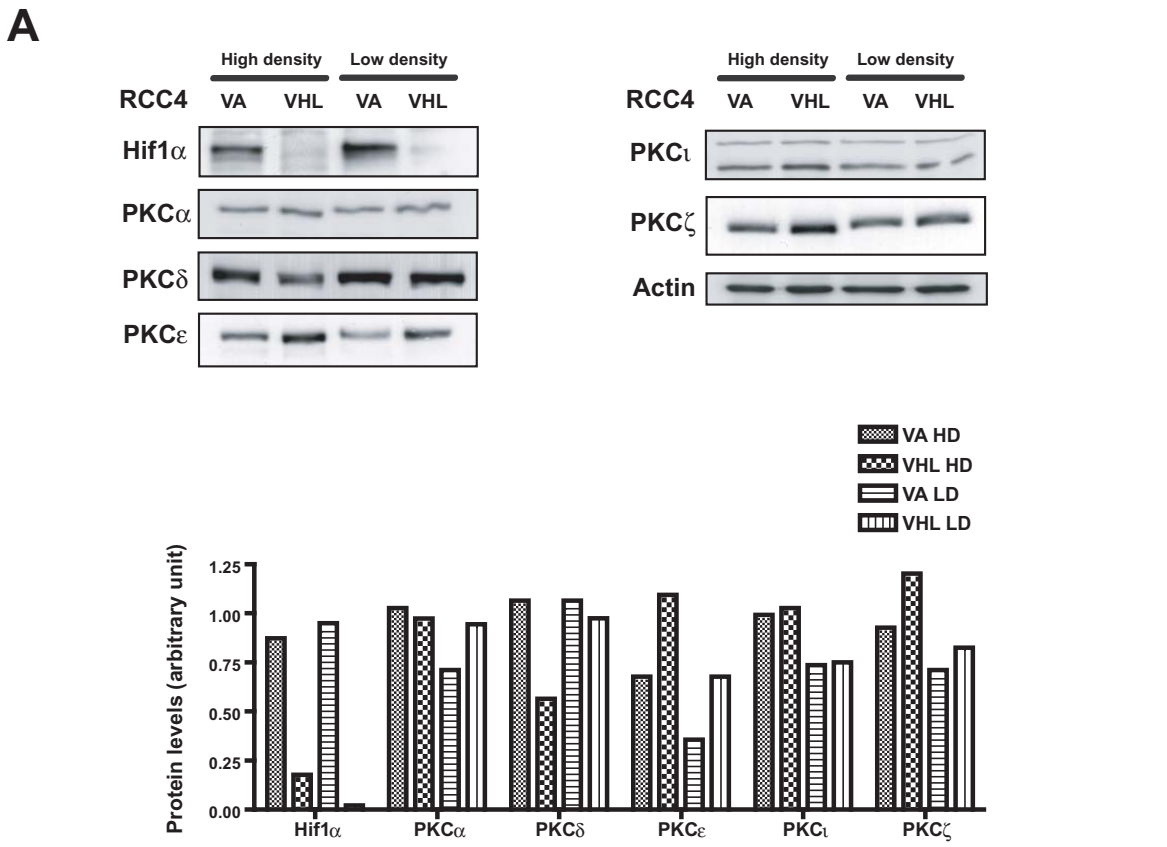

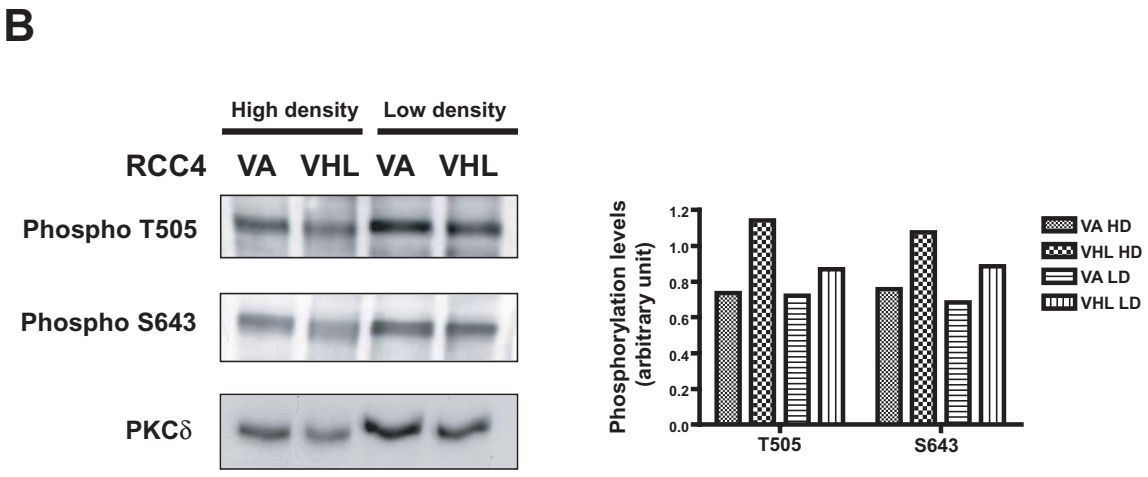

Iturrioz et al. Figure 5

Biochemical Journal Immediate Publication. Published on 2 May 2006 as manuscript BJ20060354

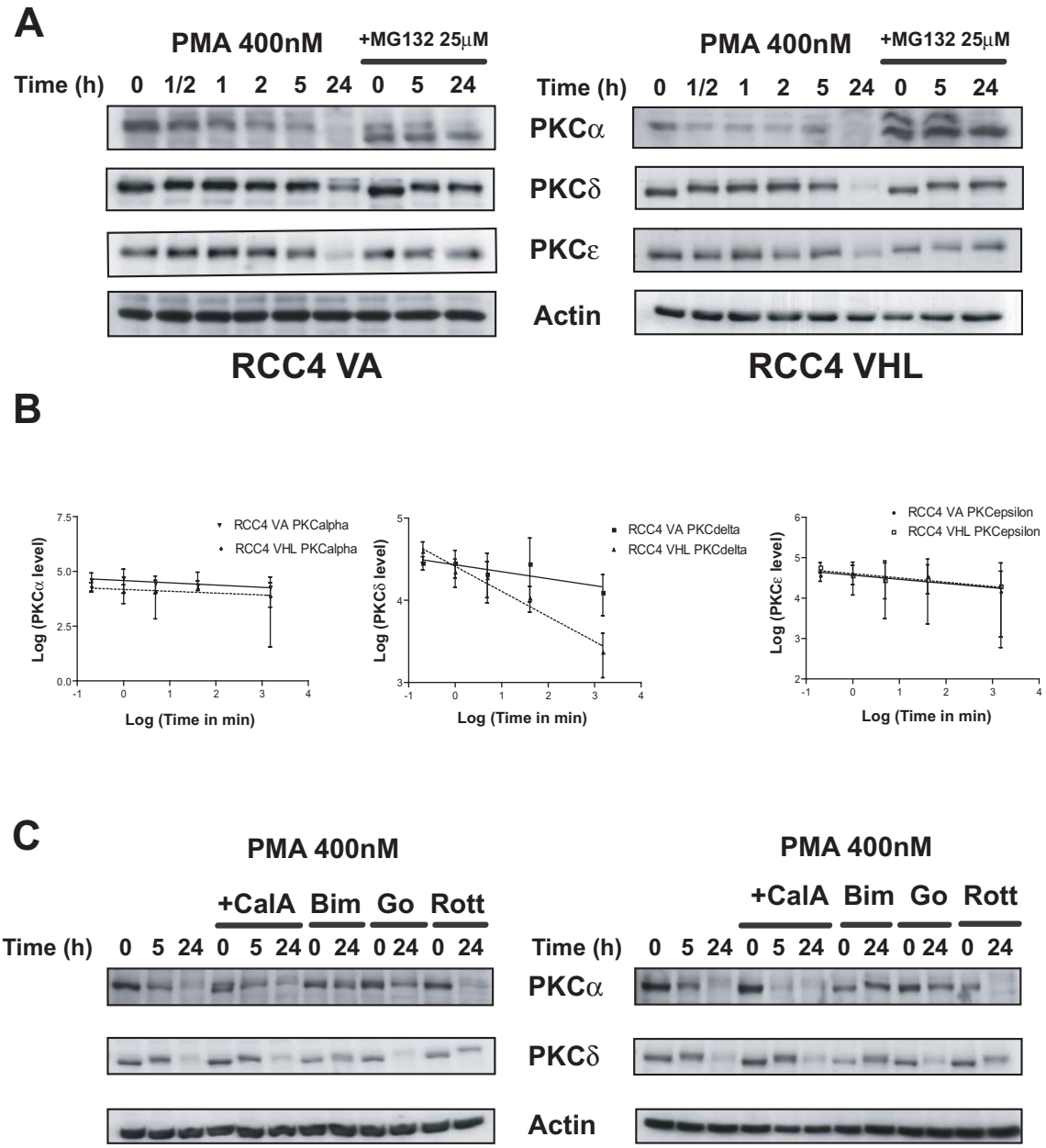

Iturrioz et al. Figure 6

Biochemical Journal Immediate Publication. Published on 2 May 2006 as manuscript BJ20060354

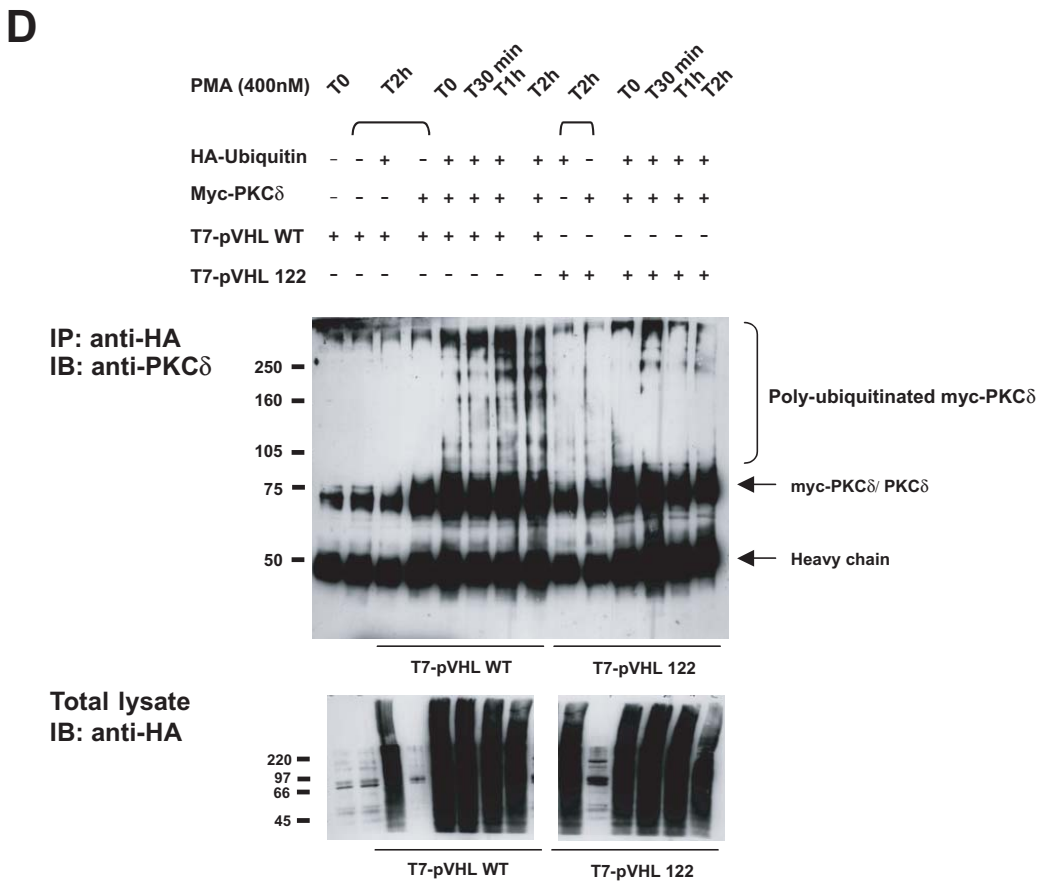

Iturrioz et al. Figure 6

Biochemical Journal Immediate Publication. Published on 2 May 2006 as manuscript BJ20060354

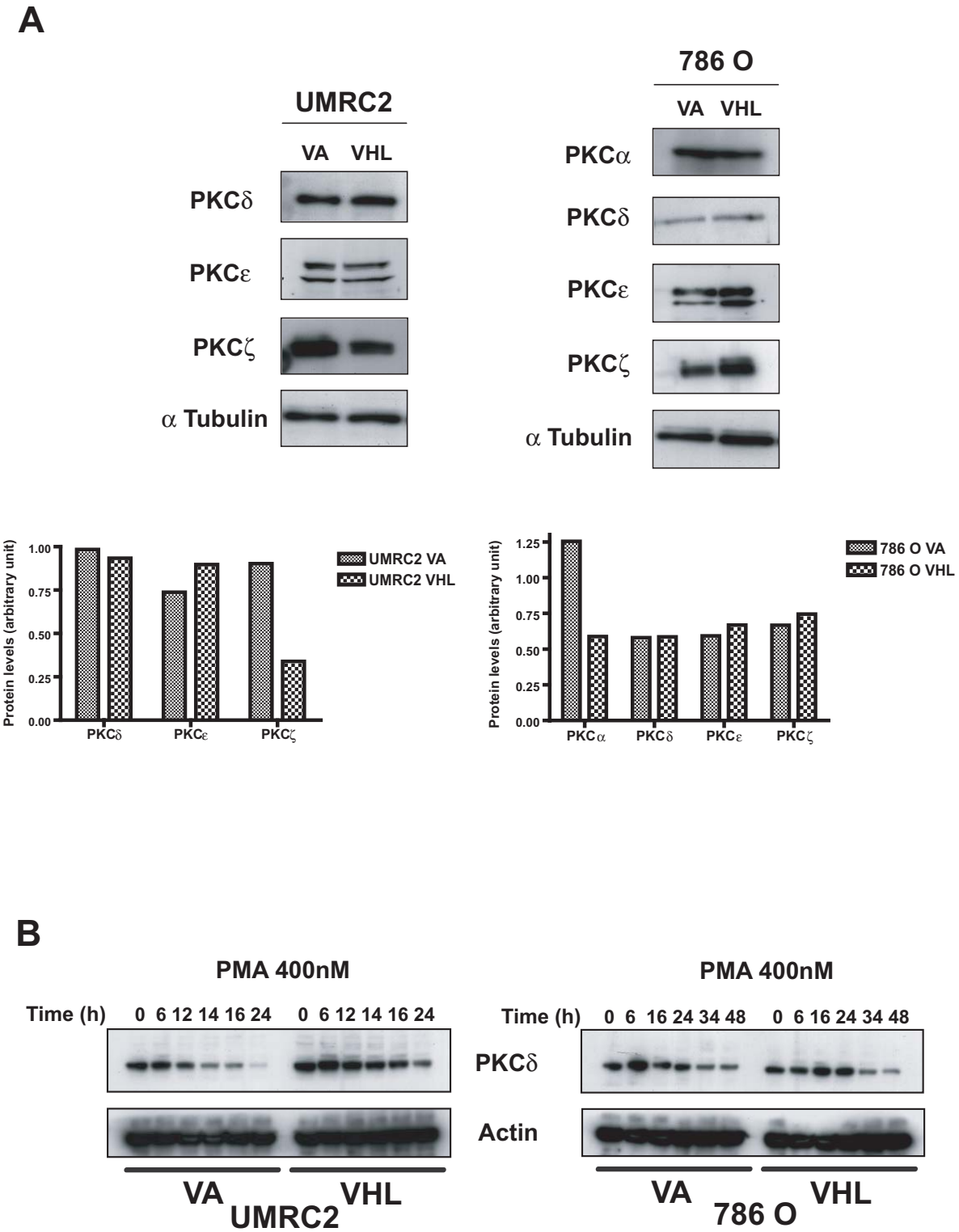

Iturrioz et al. Figure 7

Biochemical Journal Immediate Publication. Published on 2 May 2006 as manuscript BJ20060354

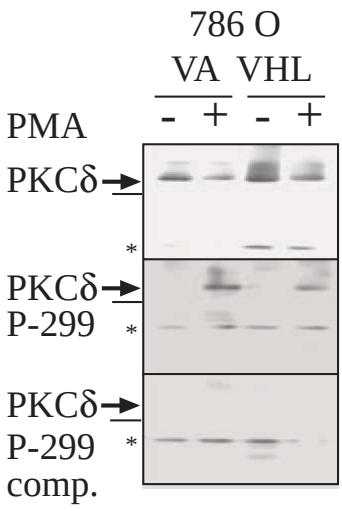

Iturrioz et. al. Figure 8